Journal of Alloys and Compounds 690 (2017) 281–286

Contents lists available at ScienceDirect

Journal of Alloys and Compounds

journal homepage: http://www.elsevier.com/locate/jalcom

Effects of Cu cluster evolution on soft magnetic properties of $Fe_{83}B_{10}C_6Cu_1$ metallic glass in two-step annealing

G.T. Xia, Y.G. Wang*, J. Dai, Y.D. Dai

College of Materials Science and Technology, Nanjing University of Aeronautics and Astronautics, Nanjing 210016, People's Republic of China

A R T I C L E I N F O

Article history:
Received 27 May 2016
Received in revised form
8 August 2016
Accepted 16 August 2016
Available online 18 August 2016

Keywords:
Cu clusters
Amorphous materials
Soft magnetic properties
Mössbauer spectra
Two-step annealing

A B S T R A C T

Not all Cu clusters in Fe-based nanocrystalline alloys can significantly influence the soft magnetic properties. In this study, a density increment of beneficial Cu clusters serving as heterogeneous nucleation sites was obtained by the two-step annealing of the $Fe_{83}B_{10}C_6Cu_1$ alloy. The formation and growth of Cu clusters during pre-annealing process were investigated by Mössbauer spectra. An increase of saturation flux density (B_S) from 1.76 T to 1.81 T and a distinct decrease of coercivity (H_C) from 8.8 A/m to 3.2 A/m were achieved by the two-step annealing. The density increment of beneficial Cu clusters is believed to be the main reason why the two-step annealed $Fe_{83}B_{10}C_6Cu_1$ alloy has an increased B_S and a decreased H_C.

1. Introduction

As energy saving has been paid more and more attention, the demanding of high performance Fe-based soft magnetic materials has become more and more eagerly. Fe-based nanocrystalline soft magnetic alloys obtained by crystallization of their amorphous precursors show high B_S and low H_C. Since Yoshizawa et al. [1] reported the first nanocrystalline soft magnetic material based on the Fe-Si-B-Cu-Nb system, continuous efforts have been made to search promising Fe-based materials with high B_S, high permeability, low H_C and low core loss. In various Fe-based nanocrystalline alloy systems such as Fe-Zr-B-Cu [2], Fe-B-Cu [3], Fe-B-Si-Cu [4], Fe-Si-B-P-Cu [5], Fe-B-C-Cu [6] and Fe-P-Cu [7], a small amount of Cu addition is necessary to promote nanocrystallization of α-Fe. Cu has a large phase separation tendency from the Fe-based amorphous matrix because of its relatively large positive mixing enthalpy (+13 kJ/mol) with Fe [8,9]. Therefore Cu atoms cluster prior to crystallization in Fe-based amorphous alloys. At the same time, a good matching between $(111)_{fcc\text{-}Cu}$ and $(011)_{bcc\text{-}Fe}$ and high concentration of Fe at the interface between Cu clusters and amorphous matrix due to Fe atoms rejecting from Cu clusters result in more heterogeneous nucleation sites [10–12]. This mechanism has been confirmed in numerous nanocrystalline soft magnetic materials such as $Fe_{73.5}Si_{13.5}B_9Nb_3Cu_1$ [13], $Fe_{89}Zr_7B_3Cu_1$ [14], $Fe_{44}Co_{44}Zr_7B_4Cu_1$ [15], $Fe_{78.8-x}Co_xNb_{2.6}Si_9B_9Cu_{0.6}$ [16], $(Fe_{0.85}B_{0.15})_{100-x}Cu_x$ [17] and $Fe_{82.65}Cu_{1.35}Si_xB_{16-x}$ [17]. However, not all the Cu clusters formed in the amorphous matrix could serve as heterogeneous nucleation sites for the α-Fe phase. Chen et al. [17] revealed that only Cu clusters with a size of 4–6 nm could increase the density of α-Fe heterogeneous nucleation sites in Fe-B-Cu alloy system.

Hence, it is reasonable to imagine that some Cu clusters exist but do not serve as heterogeneous nucleation sites of α-Fe nanocrystallization in alloy systems such as Fe-B-C-Cu. It becomes attractive to make the most use of limited Cu (about 1 at% in most alloy systems) and exhaust its potential to form Cu clusters as heterogeneous nucleation sites. In this work, with the help of Mössbauer spectra and the deduced magnetic hyperfine field distributions, increasing the density of beneficial Cu clusters which can serve as heterogeneous nucleation sites is attempted by two-step annealing to improve the soft magnetic properties of $Fe_{83}B_{10}C_6Cu_1$ alloy.

2. Experimental details

Alloy ingots of nominal composition $Fe_{83}B_{10}C_6Cu_1$ have been prepared by arc-melting of industry raw materials: Fe (99.9%), Cu (99.99%), B-Fe (B: 17%, Fe: 82.9%) and C-Fe (C: 4.43%, Fe: 95.078%).

* Corresponding author.
E-mail address: yingang.wang@nuaa.edu.cn (Y.G. Wang).

http://dx.doi.org/10.1016/j.jallcom.2016.08.150

They were remelted four times and stirred by magnetic beater to ensure the homogeneity of chemical components in a Ti-deoxidant argon atmosphere. Amorphous ribbons with a thickness of 25 μm and width of 1.5 mm were then produced by melt-spinning at an argon atmosphere onto a copper wheel with circumferential speed of 40 m/s. In the annealing process, all melt spun ribbons were sandwiched by two quartz plates to ensure the good thermal conductivity. To study the Cu cluster evolution process, the samples were pre-annealed at 548–628 K for 10 min. And then the two-step annealing experiments were carried out at a pre-annealing temperature (from 548 K to 628 K) for 10 min and subsequent 708 K for 100 s. As a reference, a conventional annealing experiment was carried out as well at 708 K for 100 s.

A differential scanning calorimeter (DSC) was employed to evaluate the thermal dynamic characteristics. Experiments have been carried out at a heating rate of 20 K/min with continuously purged argon. Structure of the melt spun and annealed ribbons was characterized using both XRD with Cu Kα radiation ($\lambda = 0.154056$ nm) at a step size of 0.02° and room-temperature Mössbauer spectroscopy with ^{57}CoRh as γ-ray source. The Normos was applied to evaluate Mössbauer spectra, which is a group of two least-squares fitting programs. In the method (also called histogram method), we define the range of the magnetic hyperfine field (B_{hf}), from 0 T to 38 T with a step of 1 T, and find the optimum histogram of sub-spectra areas for the spectrum. The calibration of Mössbauer spectra was carried out using a Fe foil of 25 μm thick and the isomer shift (IS) was also relative to the α-Fe. The forming of Cu clusters in the early stage of crystallization and the change of α-Fe volume fraction were identified by the magnetic hyperfine field distributions. B-H loop tracer with the maximum magnetizing field of 8000 A/m was used to measure the coercivity and magnetic flux density of $Fe_{83}B_{10}C_6Cu_1$ alloys.

3. Results and discussion

As shown in the XRD pattern in Fig. 1 the melt spun ribbon is at amorphous state. To determine the optimum pre-annealing condition for Cu clustering in the amorphous $Fe_{83}B_{10}C_6Cu_1$ alloy, DSC analysis was performed and curves corresponding to melt spun and pre-annealed ribbons are shown in Fig. 2. Curves except for that of the sample pre-annealed at 628 K show clearly two separated exothermic peaks marked as T_{x1} (primary crystallization temperature) and T_{x2} (secondary crystallization temperature), which correspond to the onset crystallization temperatures of α-Fe and Fe-B phases [6], respectively. The disappearance of crystallization peak corresponding to α-Fe in the sample pre-annealed at 628 K may be due to the fact that the sample has already nanocrystallized during pre-annealing process. From the DSC curve of the melt spun ribbon one can see that the T_{x1} and T_{x2} are about 710 K and 775 K. From the DSC curves of the pre-annealed ribbons, an apparent decrease of T_{x1} from 710 K to 675 K is observed, which indicates that pre-annealing promotes the precipitation of α-Fe phase. This observation agrees well with the report that pre-annealing carried out at a temperature nearly 100 K below the primary crystallization temperature leads to a better formation of Cu clusters [18,19]. Cu clusters serving as heterogeneous nucleation sites reduce the nucleation activation energy and beneficial Cu clusters obtained by pre-annealing contributes to the decrease of T_{x1}. Moreover, T_{x2} of all curves in Fig. 2 maintain about 775 K constantly, which is believed to result from the fact that pre-annealing has little effect on the nucleation of Fe-B phase. An enlarged ΔT_x ($=T_{x2} - T_{x1}$) from 65 K to 100 K expands the annealing temperature range and conduces to good soft magnetic properties of the alloy at nanocrystalline sate.

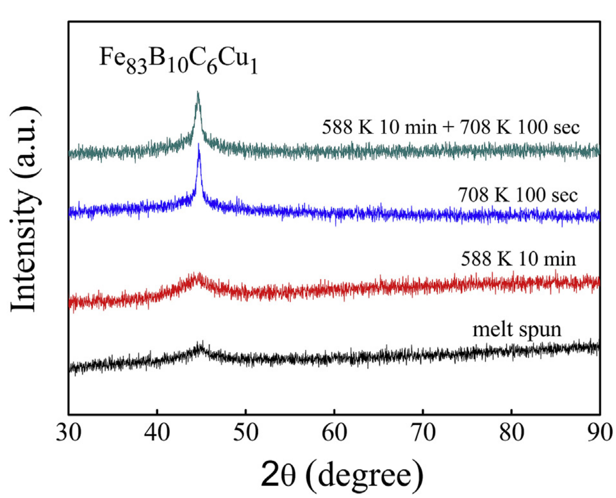

Fig. 1. XRD patterns for the melt spun and annealed $Fe_{83}B_{10}C_6Cu_1$ alloy ribbons.

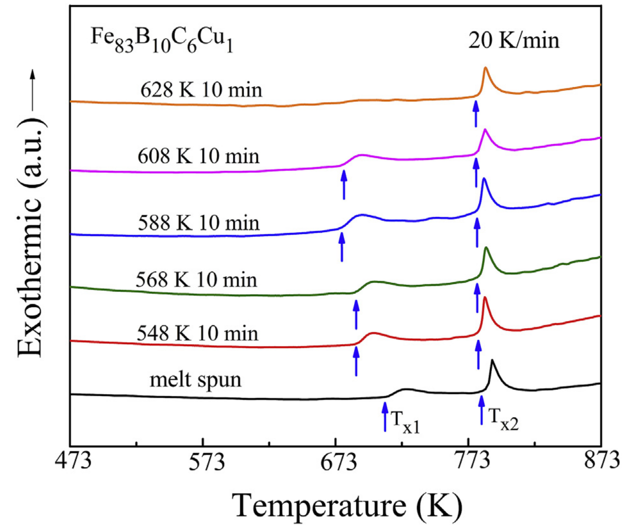

Fig. 2. DSC curves of the melt spun and pre-annealed $Fe_{83}B_{10}C_6Cu_1$ alloy ribbons.

As shown in Fig. 1, XRD patterns of both melt spun and pre-annealed (at 588 K) ribbons are with a broad peak, which is the characteristic of an amorphous phase. Sharp diffraction peak superimposed on a broad peak at about $2\theta = 45°$ corresponding to (110) of α-Fe can be detected when the ribbons were treated by conventional (708 K 100 s) and two-step (588 K 10 min + 708 K 100 s) annealing. The full width at half maximum (FWHM) of the diffraction peak in the XRD pattern of the two-step annealed ribbon is obviously larger than that of the conventional one. According to Scherrer's formula [7,20], the average grain size D can be calculated as:

$$D = K\lambda/\beta\cos\theta$$

where K is Scherrer Constant, λ is the wave length of incident X-ray ($\lambda = 1.54056$ Å), β is the FWHM of the diffraction peak, θ is the diffraction angle. Hence, the average grain size D obtained from two-step annealing (11 nm) would be smaller than that from conventional one (17 nm). From the XRD analysis, one could conclude that the two-step annealing, which comprises low-temperature pre-annealing (first-step) for forming Cu clusters with appropriate size in an amorphous matrix and a subsequent high-temperature annealing (second-step) for the α-Fe phase